Carbohydrate Polymers 95 (2013) 16–24

Contents lists available at SciVerse ScienceDirect

Carbohydrate Polymers

journal homepage: www.elsevier.com/locate/carbpol

Chitosan as matrix for bio-polymer dispersed liquid crystal systems

Luminita Marin[a,*], Maria-Cristina Popescu[a], Andrei Zabulica[a], Hiroshi Uji-I[b], Eduard Fron[b]

[a] "Petru Poni" Institute of Macromolecular Chemistry of Romanian Academy, Iasi, Romania
[b] Laboratory of Photochemistry and Spectroscopy, Department of Chemistry, KU Leuven, Celestijnenlaan 200F, 3001 Heverlee, Belgium

ARTICLE INFO

Article history:
Received 5 December 2012
Received in revised form 31 January 2013
Accepted 16 February 2013
Available online 26 February 2013

Keywords:
Chitosan
4-Cyano-4′-pentylbiphenyl
Anchoring effect
Ordering coupling at interface
Radial configuration

ABSTRACT

The obtaining of bio-polymer dispersed liquid crystal (bio-PDLC) systems based on a chitosan polymer matrix is reported here for the first time. The new PDLC composites have been obtained by encapsulation of 4-cyano-4′-pentylbiphenyl (5CB) as low molecular weight liquid crystal into chitosan, and they have been characterized by polarized optical microscopy, differential scanning calorimetry, electron and transmission scanning microscopy, Raman and fluorescence spectroscopy.

Submicrometric liquid crystalline droplets with uniform size distribution and density have been obtained for low liquid crystal content into the PDLCs. The droplets have a radial configuration being anchored into chitosan matrix by an interface ordering coupling phenomenon.

1. Introduction

Among the composite materials, polymer dispersed liquid crystal (PDLC) systems are a class of materials largely developed in the last decades due to their use in the building of a large spectrum of devices. Starting with projection displays (Kikuchi, Fujii, Kawakita, Fujikake, & Takizawa, 2000), smart windows (Liu et al., 2011), or holographic systems (Su, Chu, Chang, & Hsiao, 2011), studies on PDLC systems are continuing at present, the newest ones being directed to bring the use of the PDLC systems to bio-applications, e.g. smart food packaging (Perju, Marin, Grigoras, & Bruma, 2011) or tunable artificial iris modulating light intensity through human eyes for assisting patients of aniridia (Hsu, Lu, Huang, & Shih, 2011). To apply PDLC systems as new biomaterials for the next generation of materials for biotechnology and medicine, friendly soft composites based on biocompatible polymers need to be developed. To meet this requirement, this paper is focused on the obtaining of new PDLC systems based on chitosan as a polymer matrix.

A short overview of the literature shows that various polymeric matrices were used for the obtaining of PDLCs: poly(styrene)s (Wang et al., 2007), poly(methylmethacrylate)s (Lv, Liu, Li, Tang, & Zhou, 2012), poly(dimethylsiloxane)s (Formentin, Papacios, Ferre-Berrull, Palares, & Marsal, 2008), poly(acrylate)s and branched poly(acrylate)s (Zhou, Collard, Park, & Srinivasalao, 2002), thiol–ene polymers (White, Natarajan, Tondiglia, Bunning, & Guymon, 2007), UV curable resin NOA65 (Norland Products) (Russed, Peterson, Imrie, & Heeks, 1995), polysulfone (Marin & Perju, 2009), polyvinylalcohol and so on (Mucha, 2003), but none reports chitosan as the polymeric matrix.

Chitosan, the linear and partly acetylated (1–4)-2-amino-2-deoxy-beta-D-glucan-isolated from marine chitin (Muzzarelli et al., 2012; Muzzarelli, Jeuniaux, & Gooday, 1986) is a promising candidate as polymer matrix for bio-PDLC systems due to its outstanding intrinsic biological properties: it is biocompatibile, fungistatic, immunoadjuvant, it has the ability to improve wound healing or blood clotting (Ravi Kumar, Muzzarelli, Muzzarelli, Sashiwa, & Domb, 2004). Furthermore, chitosan meets the main requirements of polymers as components of blends or composites with liquid crystals: film forming ability, transparency, inertness in relation to a liquid crystal and immiscibility with a liquid crystal in solid state (Mucha, 2003). Moreover, chitosan can be cross-linked with a large variety of binder agents (Berger et al., 2004; Muzzarelli, 2009), increasing its potential to be used as matrix for the confinement of liquid crystal droplets.

For all these reasons, we set out to obtain new PDLC systems using chitosan as polymer matrix, by encapsulation method. As liquid crystal, 4-cyano-4′-pentylbiphenyl (5CB) has been chosen, an archetypal example of a small molecule nematic liquid crystal usually involved to obtain PDLC systems due to its technological importance (Zou & Fang, 2011).

* Corresponding author. Tel.: +40 749142080.
E-mail addresses: lmarin@icmpp.ro, lmarin2011973@yahoo.com (L. Marin).

0144-8617/$ – see front matter © 2013 Elsevier Ltd. All rights reserved.
http://dx.doi.org/10.1016/j.carbpol.2013.02.028

Table 1
Codes and component percentage of PDLC composites.

Code	C1	C2	C3	C4	C5
% 5CB	10	20	30	40	50
% Chitosan	90	80	70	60	50

2. Materials and methods

2.1. Materials

Low molecular weight chitosan, 4-cyano-4′-pentylbiphenyl 98% and acetic acid 99% were purchased from Sigma–Aldrich. The molecular weight of the chitosan was calculated to be 125 kDa and its degree of acetylation (DA) value was evaluated to be 13.5% (Brugnerotto et al., 2001; Marin, Simionescu, & Barboiu, 2012). The refractive index of chitosan ($n = 1.54$) is within the variation range of the liquid crystal 5CB ($n_o = 1.53$ and $n_e = 1.71$).

2.2. PDLC obtaining

The targeted PDLC composites were obtained by means of the encapsulation technique, when the system is heterogeneous during the whole process.

Into a 2% (w/v) chitosan solution in 0.7% acetic acid in water, a 10% solution of 5CB dissolved in chloroform was slowly dropped. During the dropping the mixture became milky. The mixture was magnetically stirred for 3 h, with 750 rot/min, at 50 °C. To reduce the size of the liquid crystal clusters and to further enhance their uniform distribution, the mixture solution was stirred by employing a vortex mixer for 5 min, every 45 min. The obtained composites were deposited onto a glass substrate and allowed to stabilize by solvent evaporation in atmospheric conditions. The composite films were dried under vacuum at 60 °C.

To perform TEM measurements, thin films of PDLC composites were casted into the pores (283 μm × 283 μm) of a 20 μm thick gold electron microscopy grid and rapidly dried under vacuum, at 60 °C.

Different weight ratios of the 5CB and chitosan were used (Table 1).

2.3. Investigation methods

The thermotropic behavior of the 5CB and PDLC films was studied by observing the textures with an Olympus BH-2 polarized light microscope, under cross polarizers, with a THMS 600 hot stage and LINKAM TP92 temperature control system.

The morphology of the films was investigated by scanning electron microscopy using a Quanta 200 ESEM, and by transmission electron microscopy using a Hitachi High-Tech HT 7700.

Differential scanning calorimetry (DSC) measurements were performed with a Pyris Diamond DSC, Perkin Elmer USA system, under nitrogen atmosphere (nitrogen flow 20 ml/min). The transition temperatures were read at the top of the endothermic and exothermic peaks. The amount of film sample was calculated to contain 3 mg of 5CB.

Confocal Raman spectroscopy was performed using an inverted microscope (TiU, Nikon) equipped with an oil immersion objective (Plan Fluor, 100×, N.A. = 1.3). 632.8 nm line from a He–Ne laser (Model 1145P, JDS Uniphase Co.) was used as the excitation source. Excitation polarization was tuned using a half-and/or a quarter-wave plates. The laser beam was guided through a dichroic mirror (z633rdc, Chroma Technology Co.) to the objective and focused to the sample plane. For Raman mapping, the sample was scanned using a moving piezo stage. The Raman scattering was collected by the same objective and passed through a spatial pinhole (100 μm in diameter) to realize a confocal detection condition followed by a special filter (HQ645LP, Chroma Technology Co.) and guided to a spectrograph (Shamrock303 equipped with 600 graves/mm reflective grating, Andor Technol.) equipped with a CCD camera (Newton, Andor Technol.). Raman mapping measurements were carried out using an atomic force microscopy (AFM) instrument synchronized with the Raman spectrograph (Combiscorp, AIST-NT). The Raman data were collected at room temperature (22 °C). The spectra are recorded in the range 500–2500 cm^{-1} with a spatial resolution of 0.2 mm. All spectra were fitted with a Lorentz function and processed with a linear baseline. The color-coded images (i.e. plots of spectral parameter versus the *X*–*Y* coordinates of the respective sampling point) are produced with Matlab software, providing the spatial intensity distribution of the ν(CN) or ν(CC) Raman bands of a chosen area on the PDLC sample. The collected band intensities depend on the orientation of the molecules, and most of the physical structure appears in the Raman intensity map.

UV–vis absorption and photoluminescence spectra were recorded on a Carl Zeiss Jena SPECORD M42 spectrophotometer and a Perkin Elmer LS 55 spectrophotometer, respectively, in solution and film, using 10 mm quartz cells or glass plates.

3. Results and discussions

Five new PDLC composites, named C1–C5, based on chitosan as polymer matrix and 4-cyano-4′-pentylbiphenyl (5CB) as liquid crystal were obtained for the first time, by means of encapsulation, using different weight ratios between the two components (Table 1). The composites gave free standing flexible films. Polarized light optical microscopy (POM), electron scanning microscopy (SEM), transmission scanning microscopy (TEM), Raman spectroscopy and differential scanning calorimetry (DSC) were used as complementary methods to evidence liquid crystal droplet formation, their configuration, anchoring effect and morphologic stability of the new composites.

3.1. Polarized optical microscopy

Observing the composite film samples by POM at room temperature revealed liquid crystalline droplets for the composites with low content of 5CB (C1 and C2). The droplets are uniformly dispersed on the entire surface and show narrow size dispersity (Fig. 1a). In the case of composites with higher liquid crystal content, a fine birefringent texture (Fig. 1b) is observed, instead of the clear segregation of the nematic droplets. This fine texture was reported also for other PDLC composites and was demonstrated to be the visual result of droplet multiple overlaps across the film thickness (Hironobu, Osamu, & Keiichiro, 2004; Liu et al., 2011; Lovinger, Amundson, & Davis, 1994; Marin & Perju, 2008, 2009; Perju et al., 2011).

By heating the samples with 5 °C/min, the 5CB droplets isotropization occurred progressively; starting with the largest droplets and finishing with the smallest ones. The spherical isotropic 5CB domains remained surrounded by a lighter shadow (Fig. 1c), indicating the ordering of the chitosan matrix around the 5CB droplets. In the subsequent cooling scan was observed the same behavior as in the heating cycle, but inverted; the smallest liquid crystal droplets appeared firstly, followed by the occurrence of larger droplets. In fact, the larger droplets were formed by the coalescence of some smaller droplets which appeared firstly. Upon applying successive heating/cooling scans, the isotropization and isotropic-to-nematic transitions occurred in the same manner, pointing to immiscibility of the PDLC components and thus to their morphological stability.

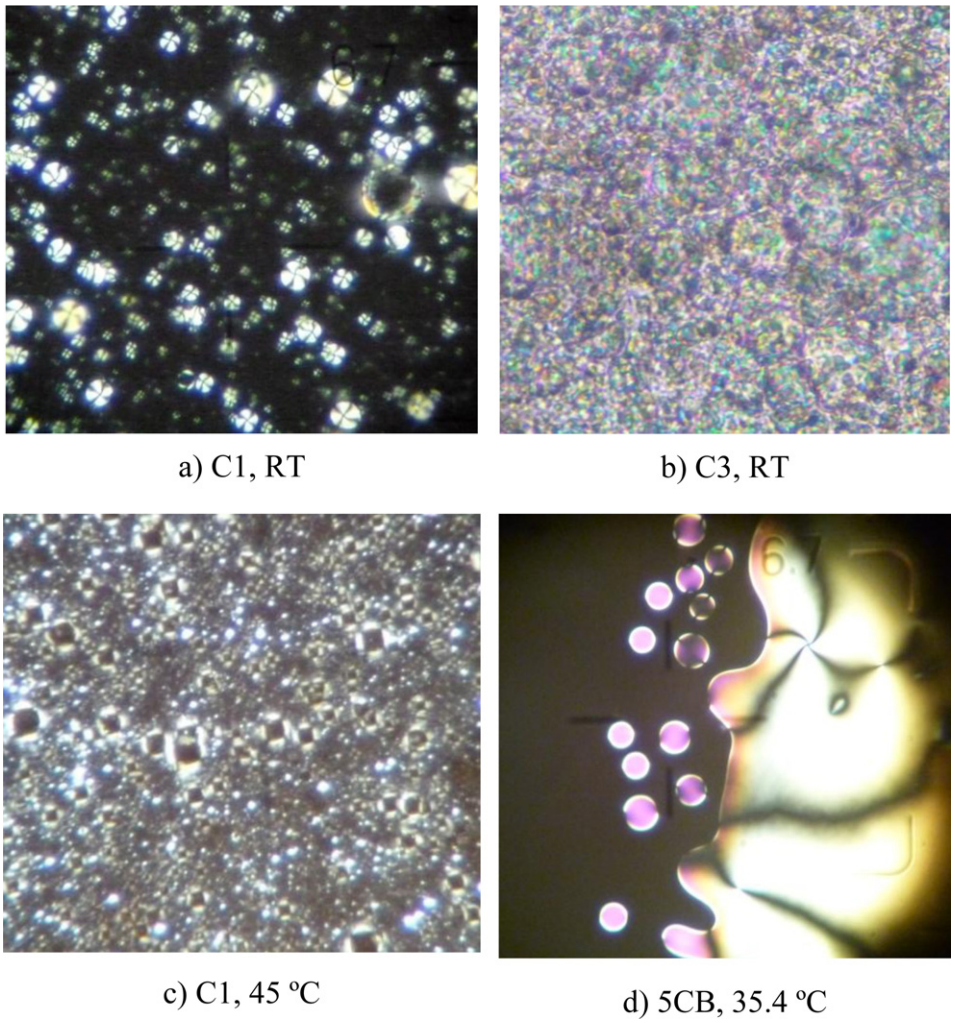

Fig. 1. Polarized light microscopy microphotographs of 4-cyano-4′-pentylbiphenyl and composite films. (a) C1, RT; (b) C3, RT; (c) C1, 45 °C; and (d) 5CB, 35.4 °C.

Usually, the liquid crystals in the PDLC systems form bipolar or radial droplets. In the radial configuration, the liquid crystal molecules are anchored with their long axes perpendicular to the droplet walls, creating one point defect in the center. The bipolar configuration occurs when the liquid crystal molecules are oriented parallel to the surface, creating two point defects (Demus & Richter, 1978). The type of droplet configuration is determined by the anchoring forces, and thus by the polymer matrix. Most polymers tend to induce a parallel alignment of the nematic director to the interface, and hence, bipolar droplets are most often found in PDLC systems (Zhou et al., 2002).

The anchoring effect of chitosan upon the 5CB was clearly revealed by the droplet configuration changes from pure liquid crystal to when embedded in polymer matrix. The pure 5CB showed bipolar nematic droplets with two surface point defects during nematic/isotropic and isotropic/nematic transition, droplets which formed a Schlieren texture with four and two brushes, by coalescence, as can be observed in Fig. 1d. On the other hand, the 5CB molecules within the PDLC droplets exhibited optical characteristics indicative of a radial configuration where the point defect was placed in the center; no bipolar droplets were observed (Fig. 1a). Moreover, the larger droplets formed by coalescence of small bipolar droplets adopted a radial configuration, also. This means that the natural tendency of the 5CB molecules to align parallel to the droplet wall in the pure 5CB changes when 5CB is encapsulated into chitosan. The radial configuration indicates that 5CB molecules are anchored with their long axes perpendicular to the droplet walls, most probably due to the attraction forces between the strongly electron withdrawing cyan end-groups of the 5CB and the protonated chitosan macromolecules. The antagonistic charges of the two components facilitate the coupling between the 5CB and chitosan macromolecules orderings. This is the reason why the lighter shadows around the LC droplets can be seen in POM after the 5CB isotropization, indicating the ordering of the chitosan macromolecules around the LC droplets. All these observations lead to the conclusion that the 5CB molecules have a homeotropic alignment inside the LC droplets, resulting in a radial structure with the point defect in the center. The radial droplets are anchored into the chitosan polymer matrix due to the phenomenon of ordering coupling at the interface.

3.2. Scanning and transmission electron microscopy

The morphological observation was carried out by SEM techniques for the film samples resulted from removing liquid crystal with methanol. The first remarkable observation was that the 5CB forms spherical droplets inside the chitosan matrix. This indicates that the interfacial tension between chitosan and 5CB is low enough to transfer the shear stress from the matrix to the 5CB and not cause droplet deformation. Thus, the chitosan is able to act as polymer matrix in the obtaining of PDLC systems.

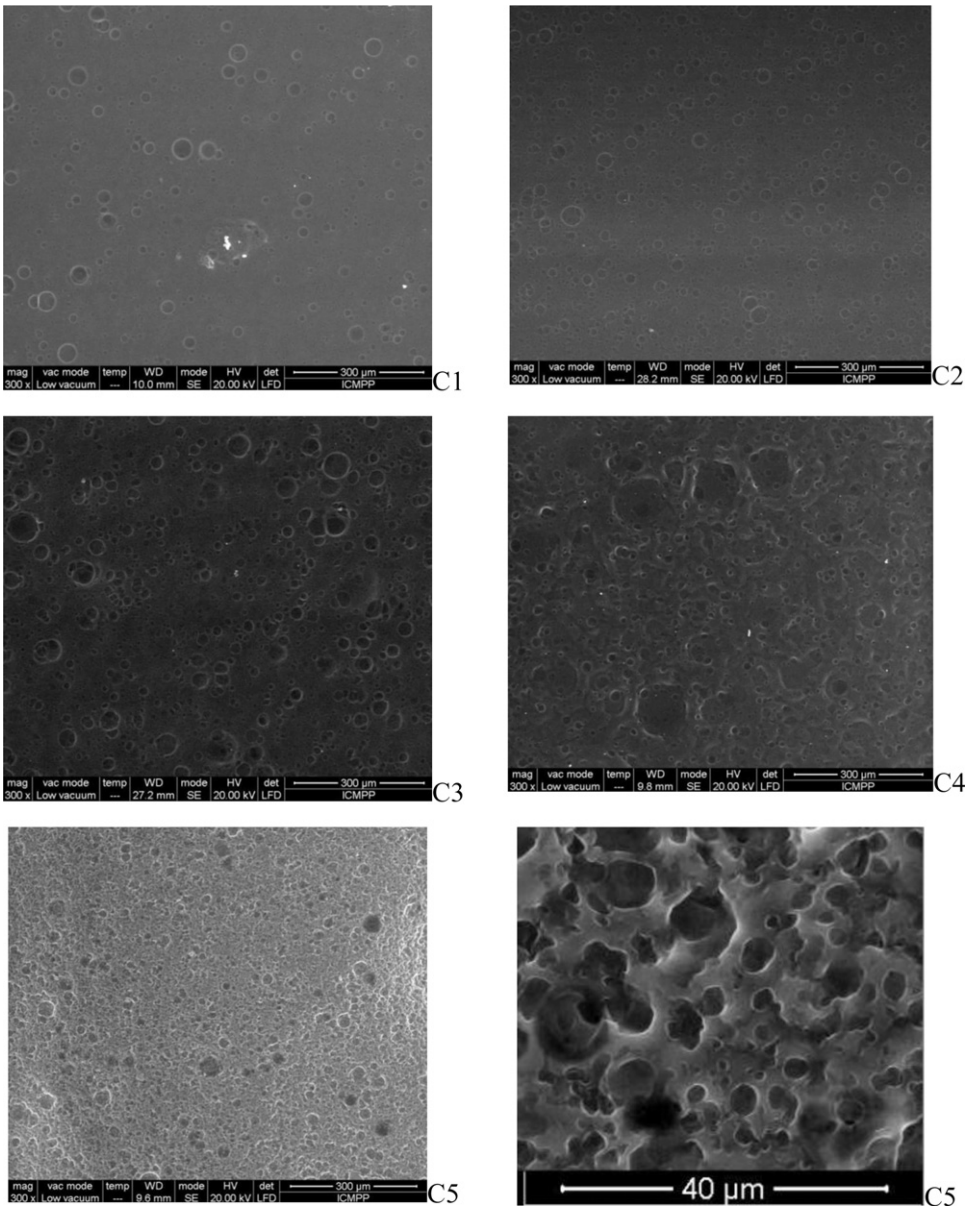

Fig. 2. Scanning electron microscopy microphotographs of the studied composites.

As it was expected, depending on the liquid crystal content, there are clear differences in droplet distribution, as they are rare for liquid crystal lower content and dense for a higher content (Fig. 2). While the chitosan film is smooth (Khan et al., 2012), the residual PDLC composites after removing the 5CB exhibit pores whose size is between 40 μm and 300 nm. The film morphology is quite regular, the cavities are independent and only in the case of the C5 composite some fused ones appear, indicating droplet collisions due to their high concentration. The 50:50 weight ratio of 5CB:chitosan seems to be the maximum content of liquid crystal in the case of the chitosan-based PDLCs. Most of the reported PDLC studies are performed on 50:50 composites, because a part of liquid crystal do not segregates in droplets but is miscible with the polymer matrix giving a "polymer rich matrix" (Formentin et al., 2008; Hadjichristov, Marinv, & Petrov, 2011; Hsu et al., 2011; Ren, Fan, Lin, & Wu, 2005; Wang et al., 2007); the mixing of liquid crystal and polymer decrease glass transition of the polymer matrix and hinder the reaching of the best optical properties of their PDLCs. The lower liquid crystal maximum content for the present chitosan-based PDLCs indicates to a maximum phase separation of the two components, which precludes the loss of liquid crystal as plasticizer into the polymer. This characteristic is further important, pointing for improving optical properties of chitosan-based PDLCs.

Upon comparing the morphology of the PDLC films in terms of shape and size no significant changes are observed. This allows to speculate that the phase separation dynamics significantly depends on the obtaining conditions and their further modification – stirring speed, temperature, evaporation rate, using of cross-linking agents of chitosan which favor the droplet frozen once the polymer matrix reaches its gelation point, use of branched chitosan (Zhou et al., 2002), using mixing of the liquid crystal with a mesogen containing a tetra(ethyleneglycol) tail in order to stabilize the emulsion droplets, to hinder the droplet coalescence and thus to increase their stability (Zhongqiang et al., 2010) – can lead to the targeted morphology.

In order to confirm this, TEM measurements on very thin films obtained by fast evaporation of the solvent were performed. Interestingly enough, TEM images reveled smaller droplets compared

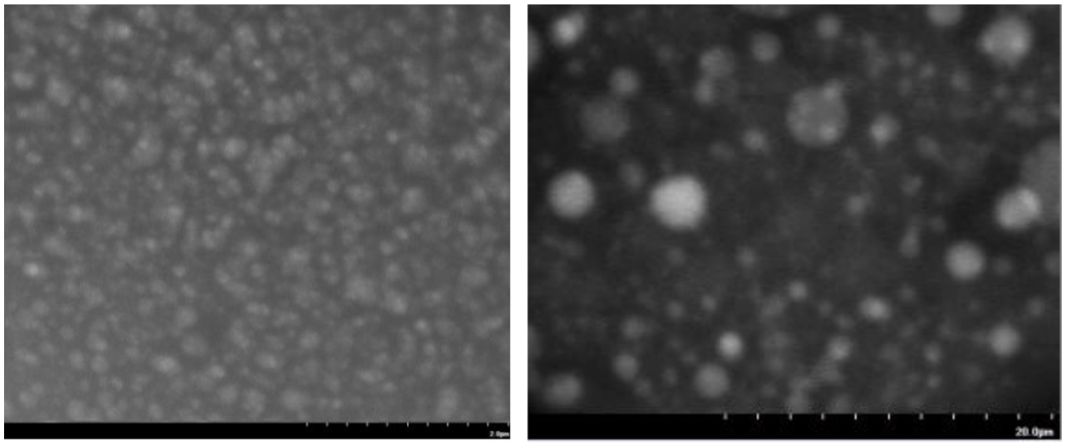

Fig. 3. Transmission electron micrographs of the composite films. The light circles represent the spherical LC droplets.

with the SEM ones – around 200 nm in diameter for the films containing a small amount of liquid crystal (C1 and C2), and around 2 μm for the films containing a larger amount of 5CB (C3 and C4) (Fig. 3). The droplets are quite uniformly distributed, especially for the C1 and C2 composites.

Upon comparing the SEM and TEM images we can conclude that the system morphology is controlled by the solvent evaporation rate. In the case of the composite films prepared for TEM measurements dried under vacuum and elevated temperature, the evaporation rate was sufficiently fast to reduce the LC droplets coalescence.

3.3. Raman scattering

Polarized optical microscopy (POM) was used in order to provide two-dimensional information about the size, shape, location, and movement of the objects in the observation plane. Raman microscopy (RM) provides yet richer information in comparison with many other imaging techniques. Since RM proves the interactions of individual bond vibrations with laser light, it presents more detailed insight into the chemical composition of the sample. In addition, the quantitative imaging of Raman intensity reveals information about the spatial organization of the molecules and their local environment. In the particular case of PDLCs, RM is used to image the director fields of liquid crystal molecules **n** in the horizontal plane and along the vertical direction (Blach, Daoudi, Buisine, & Bormann, 2005).

Uniaxial 5CB cyanobiphenyl liquid crystal molecules are very strong Raman scatterers. In the Raman spectra of this compound four bands can be evidenced at 1180 cm^{-1}, assigned to aromatic CH in-plane deformation, 1286 cm^{-1} to C—C stretching of the biphenyl link, 1606 cm^{-1} to C═C stretching of the aromatic rings and 2228 cm^{-1} to C≡N stretching (Buyuktanir, Zhang, Gericke, & West, 2008; Kachynski, Kuzmin, Prasad, & Smalyukh, 2008). The assignment of such modes has been performed by taking into account the fact that biphenyl belongs to the C2v point group and their skeletal vibrational modes can be described in four symmetry species (Castriota et al., 2011). According to this assumption, the vibrations at 1184, 1609 and 2228 cm^{-1} occur in the molecular plane, while all other vibrations occur out of the molecular plane.

The components of the optical polarizability tensor for molecules which belong to point group C2v are, in principle, all different. However, due to the rotational isotropy around the long molecular axis (*z*-axis), the optical polarizability tensor, can be represented by an oblate ellipsoid. The symmetric stretching of the aromatic rings in the biphenyl molecules and the stretching of the CN groups induce the major change of polarizability along the long molecular axis of the biphenyl molecules.

The average orientation of the cyanobiphenyl LC molecules can be evidenced by using a linear polarized laser beam and by analyzing the C≡N stretching vibrational band at 2228 cm^{-1} and the C═C stretching vibration of aromatic rings band at 1606 cm^{-1}, because the cyano-vibration is highly polarized and the direction of this vibration is parallel to the mean director direction. When the electromagnetic vector of an incident plane polarized light **P** lies along the long axis of the cyanobiphenyl compounds, the intensities of the bands associated to these vibrations are maximal and minimal when the polarization of the pump beam is perpendicular to the director. The behavior study of these bands as a result of polarized light interaction gives a useful tool to probe the director distribution.

The Raman images generated by plotting the variation of the scattering bands at 1606 and 2228 cm^{-1} illustrate the relative distribution of the 5CB within the chitosan matrix. The phase separated structure clearly exists in the sample region. The dark zones indicate the chitosan regions, while the bright zones indicate the 5CB regions. From Fig. 4 one can see that the chitosan regions are presented as a broad continuous phase, while the 5CB regions are dispersed as islands. The domains of the dispersed phase present an irregular spherical distribution with sizes between 2 and 25 μm

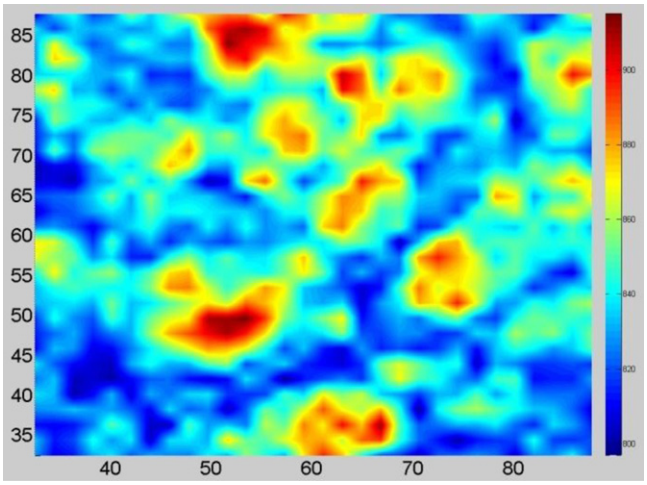

Fig. 4. Raman image (55 μm × 55 μm) of C4 composite.

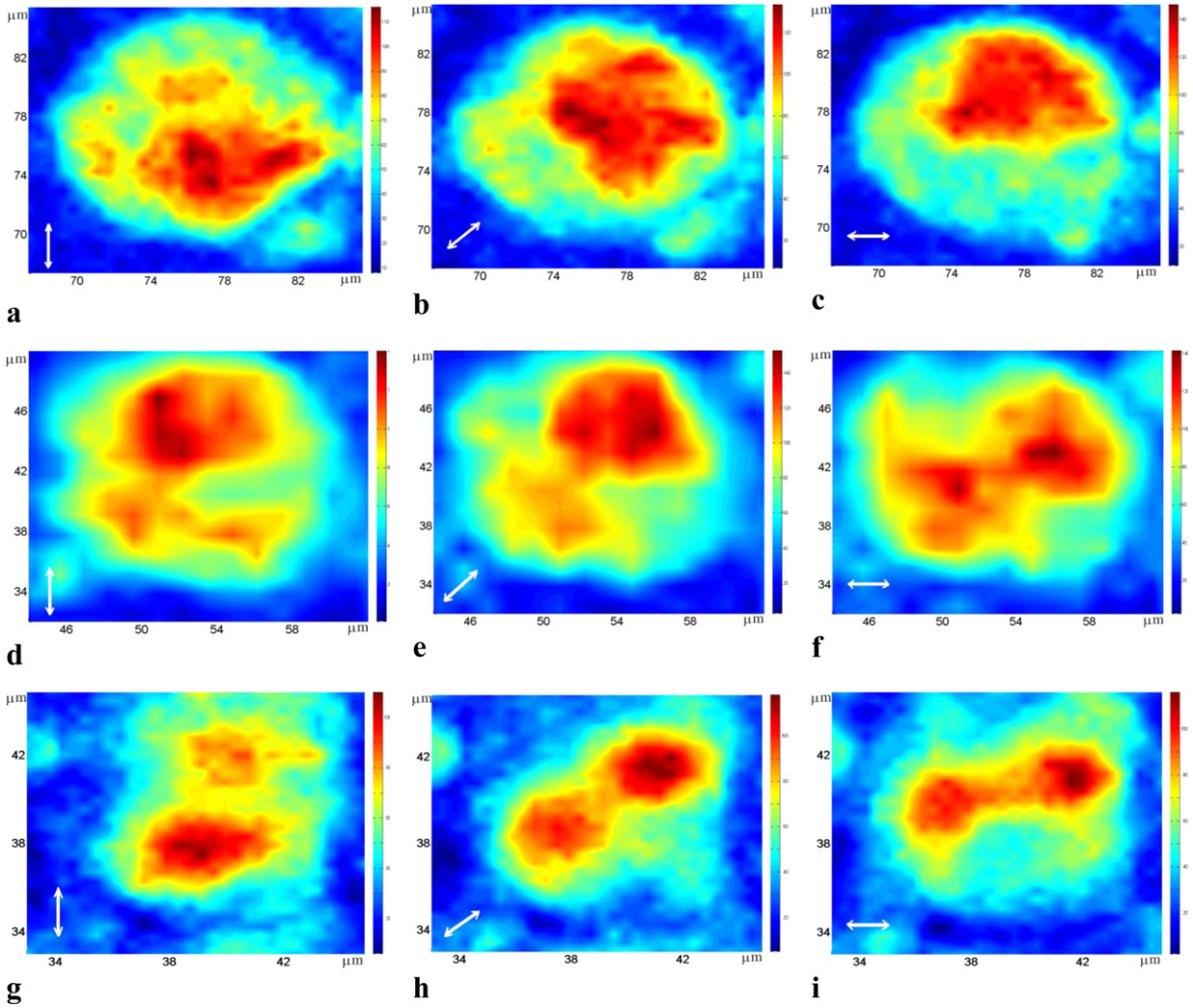

Fig. 5. Raman mapping of spatial distribution of 4-cyano-4′-pentylbiphenyl molecules in the droplets in polarized light of C3 (a–c), C4 (d–f) and C5 (g–i) for 3 directions of the polarizer (**n** || **P**, 45° between **n** and **P** and **n** ⊥ **P**).

depending on the content of 5CB in the chitosan matrix. A clear transition interface between the 5CB and the chitosan regions and also a slight diffusion of the 5CB molecules in the chitosan matrices are observed.

Fig. 5 clearly evidences a preferential orientation of the director of the 5CB molecules. The ratio of the maximum signal to the minimum signal is ~10, indicating that the C≡N and C=C groups are well aligned along the director. The color scale on the Raman images shows the change in the orientation of the ν(C≡N) stretching band. For all PDLC systems, the maximum intensity of the Raman band is located in the regions where **n** ∥ **P**, and the minimum intensity is located in the regions where **n** ⊥ **P**. As can be seen, the maximum intensity for all samples depends on the direction of the polarizer and is maximum in this direction, indicating a radial orientation of molecules in the droplets (Fig. 5). The director configuration can be correlated with the sample birefringence, which gives a unique signature to the electro-optical properties of the structure as a function of the polarization direction of the probe beam. The chemical sensitivity of Raman spectroscopy allows a detailed microscopic view of the director configuration. The Raman mapping of a large area of the sample could be conveniently used to deduce its birefringence distribution. The Raman anisotropy (A) can be defined as $A = (I_{||} - I_{\perp})/(I_{||} + I_{\perp})$, where $I_{||}$ and $I_{\perp}$ represent the band intensities of the C=C or C≡N stretching vibration parallel and perpendicular to the polarized light direction, respectively. The obtained values for all images are between −0.89 and 0.89 indicating once more a radial distribution of the 5CB molecules.

As a result, the polarized confocal microscopy confirms the POM observations, indicating the clear phase separation of 5CB droplets with a three-dimensional radial configuration.

3.4. Calorimetric studies

The investigation of PDLC systems in a wide temperature range make possible to analyze the dependence of their standard thermodynamic properties with their composition and structure and to evidence the transition temperature and/or the interactions between components. The knowledge of these properties allows the establishing the application field.

DSC thermograms of the obtained PDLCs and pure 5CB were recorded in order to gain information related to phase separation, droplet formation, liquid crystal–chitosan matrix miscibility and morphological stability (Russed, Pateron, Imrie, & Heeks, 1995; Smith, 1993). In order to compare the DSC data of the PDLC composites and the 5CB, the same measurement parameters were used. Because thermal transitions are usually strongly affected by the heating/cooling ratio, an optimal DSC temperature program was adopted, that is: cooling with 1 °C/min up to −30 °C and heating

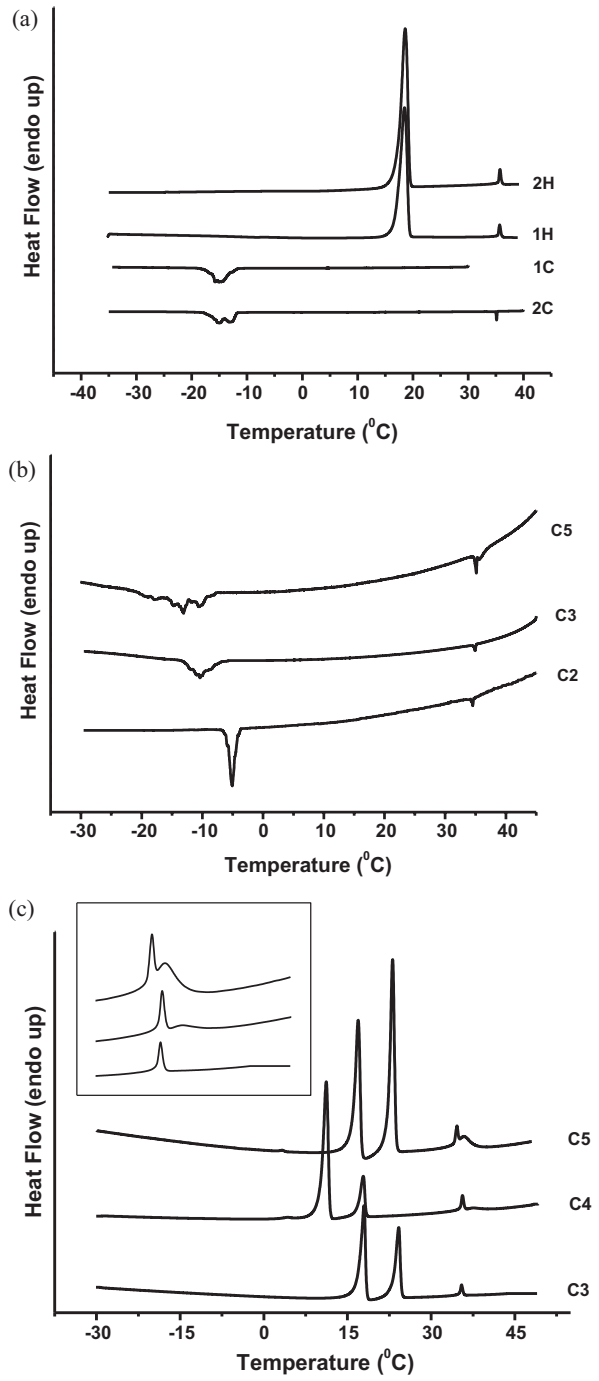

Fig. 6. Differential scanning calorimetry thermograms of 4-cyano-4′-pentylbiphenyl and studied composites. (a) DSC thermogram of 5CB (H: heating; C: cooling); (b) second DSC cooling scan of PDLCs; and (c) second heating scan of PDLCs.

with 5 °C/min up to 50 °C. This cooling/heating rate allowed a complete crystallization of the liquid crystal and a high enough temperature stability range of the nematic mesophase (Fig. 6a). Thus, in the first cooling scan starting from room temperature, a broad exothermic peak around −10 °C corresponds to the complete crystallization. In the first heating scan, an intense, sharp endothermic peak at 18.5 °C – ascribed to the crystallin–nematic transition and a weak sharp endothermic peak at 35.8 °C – attributed to isotropization were evidenced. In the second cooling scan, a sharp exothermic peak at 35.1 °C corresponds to the isotropic–nematic transition and a broad exothermic peak around −14 °C accounts for crystallization. The further heating/cooling scans are similar to the 1H/2C scans.

Compared to the pure 5CB, in the PDLC cooling scans, the exothermic peak corresponding to crystallization is sharper for the composites containing a lower percentage of liquid crystal and broader for the ones containing a higher percentage. Besides, the crystallization temperature (T_{Cr}) is higher (Fig. 6b). The increasing T_{Cr} reflects the influence of the chitosan matrix upon the 5CB micrometer-sized droplets, matrix which acts as crystallization germ facilitating the earlier ordering into crystalline state. The sharper exotherm indicates a faster crystallization due to the micrometric dispersion of droplets with an increased interface to the chitosan matrix. The broader exotherm, close in shape to the 5CB one is related to LC droplet coalescence, which decrease the 5CB/chitosan interface and thus increase the bulk liquid crystal characteristics. This behavior sustains the hypothesis of interface coupling between chitosan macromolecules organization and liquid crystal ordering; the crystallization is faster for the composites containing a smaller amount of 5CB dispersed in smaller droplets, and slower for the composites containing a larger amount of 5CB dispersed in larger droplets. The hypothesis is also supported by the evolution of the small exothermic peak ascribed to the isotropic–nematic transition. The peak is broader for PDLCs composites compared to pure 5CB liquid crystals and in particular for composites containing a larger amount of 5CB compared to those containing a smaller amount of 5CB – corresponding to the progressive appearance of nematic droplets function of their size, which reflects the influence of anchoring effect of the chitosan matrix and the 5CB droplet size dispersion.

The first DSC heating scan of the PDLC composites reveals significant changes compared to the pure 5CB one, as well (Fig. 6c). Firstly, corresponding to the crystalline–nematic transition, multiple endotherms ranging between 11 and 25 °C took the place of the sharp one in pure 5CB DSC curve, reflecting size polydispersity of the polymorphic crystallites into PDLCs. Secondly, the sharp small endotherm corresponding to the pure 5CB isotropization became broad for the 5CB into PDLCs, especially for those containing larger 5CB amounts and intriguingly, its ending point is shifted around 4 °C at higher values, around 40 °C. Compared to the most studied PDLCs whose isotropization temperatures (T_i) decrease, the formerly mentioned behavior is rather unusual. Taking into account the POM measurements which indicate a progressive transition of the nematic droplets to the isotropic state as a size function, the increase of the T_i is attributed to the stabilizing effect of the chitosan matrix upon the nematic mesophase into droplets. This unusual stabilizing effect could be reasonably ascribed to the interface connection of the 5CB and chitosan matrix and, on the other hand, to the thermal inertness of the chitosan which acts as a thermal insulator.

The further cooling/heating cycles are almost similar to the first one, indicating the immiscibility of the liquid crystal and chitosan matrix and on the other hand the PDLC morphological stability. DSC measurements indicate undoubtedly the phase separation and sustain the interface connection of the 5CB and chitosan.

3.5. Photoluminescence behavior

The 5CB liquid crystal is known to be a fluorescent compound with weak absorption in the visible spectral region. Due to its use in composite obtaining, many studies have been dedicated to the investigation of its photophysical properties, concluding that the 5CB spectral changes are connected with the formation and destruction of different monomer and dimer structures of the 5CB molecules and also with their conformational changes (Bezrodna, Melnyk, Vorobjev, & Puchkovska, 2010; Piryatinski & Yaroshchuk, 2000). To see how the confinement of the 5CB in the chitosan matrix

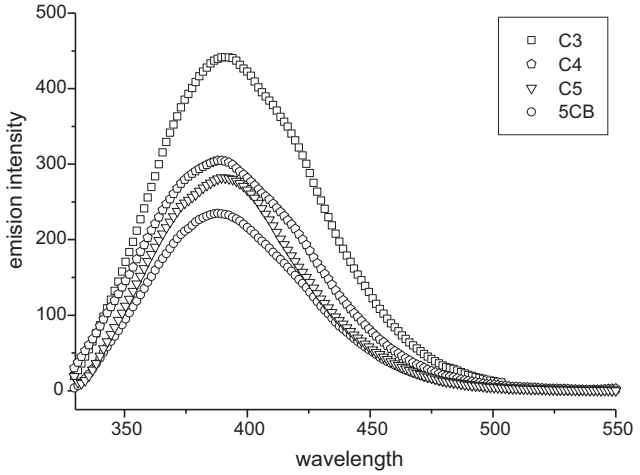

Fig. 7. Photoluminescence spectra of 4-cyano-4′-pentylbiphenyl in PDLC composites, at room temperature.

affects its photophysical characteristics, the fluorescence spectra of the PDLC films were recorded, by exciting them with λ_{ex} = 315 nm (Bezrodna et al., 2010).

As with 5CB, all the PDLC spectra had the same shape and emission maximum, but their intensity increased for the composites containing a smaller amount of liquid crystal (Fig. 7). This means that the dispersion of liquid crystal in smaller droplets improves its emission properties. The change of the 5CB luminescence under the influence of the chitosan matrix can be explained by the interphase interaction which leads to a better conjugation and thus a flatter conformation of the 5CB molecules into the radial droplets. Smaller droplets means larger interphase surface and as a consequence, higher luminescence intensity.

4. Conclusions

PDLC composites based on chitosan matrix and 5CB liquid crystal have been successfully obtained for the first time by encapsulation method. The micron-size droplets were obtained by air-evaporation and submicron-size droplets were obtained by thermal evaporation under vacuum. The chitosan matrix generates the homeotropic alignment of the liquid crystal due to the positive charge of its protonated state. The nematic liquid crystal droplets have a radial configuration with the point defect in the center. They are stabilized into the chitosan matrix due to the phenomenon of ordering coupling at interface.

The chitosan-based PDLCs formation results in an increasing luminescence ability of the 5CB, due to its micronic dispersion which leads to an increase of the surface.

A very important conclusion of this study is that using chitosan as polymer matrix offers the possibility to obtain PDLC films containing a small amount of liquid crystal.

Acknowledgements

The financial support of European Social Fund – "Cristofor I. Simionescu" Postdoctoral Fellowship Programme (ID POSDRU/89/1.5/S/55216), Sectoral Operational Programme Human Resources Development 2007–2013 is acknowledged.

References

Berger, J., Reist, M., Mayer, J. M., Felt, O., Peppas, N. A., & Gurny, R. (2004). Structure and interactions in covalently and ionically crosslinked chitosan hydrogels for biomedical applications. *European Journal of Pharmaceutics and Biopharmaceutics*, *57*, 19–34.

Bezrodna, T., Melnyk, V., Vorobjev, V., & Puchkovska, G. (2010). Low-temperature photoluminescence of 5CB liquid crystal. *Journal of Luminescence*, *30*, 1134–1141.

Blach, J-F., Daoudi, A., Buisine, J-M., & Bormann, D. (2005). Raman mapping of polymer dispersed liquid crystal. *Vibrational Spectroscopy*, *39*, 31–36.

Brugnerotto, J., Lizardi, J., Goycoolea, F. M., Arguelles-Monal, W., Desbrieres, J., & Rinaudo, M. (2001). An infrared investigation in relation with chitin and chitosan characterization. *Polymer*, *42*, 3569–3580.

Buyuktanir, E. A., Zhang, K., Gericke, A., & West, J. L. (2008). Raman imaging of nematic and smectic. *Molecular Crystal & Liquid Crystal*, *487*, 39–51.

Castriota, M., Fasanella, A., Cazzanelli, E., De Sio, L., Caputo, R., & Umeton, C. (2011). In situ polarized micro-Raman investigation of periodic structures realized in liquid-crystalline composite materials. *Optics Express*, *19*, 10494–10500.

Demus, D., & Richter, L. (1978). *Textures of liquid crystals*. Leipzig: VerlagChemie, Weinheim.

Formentin, P., Palacios, R., Ferre-Berrull, J., Pallares, J., & Marsal, L. F. (2008). Polymer-dispersed liquid crystal based on E7: Morphology and characterization. *Synthetic Metals*, *158*, 1004–1008.

Hadjichristov, G. B., Marinov, Y. G., & Petrov, A. G. (2011). Gradient polymer-dispersed liquid crystal single layer of large nematic droplets for modulation of laser light. *Applied Optics*, *50*, 2326–2333.

Hironobu, H., Osamu, U., & Keiichiro, A. (2004). Dielectric relaxation in phase-segregated mixtures of polystyrene and liquid crystal 5CB. *Macromolecules*, *37*, 1583–1590.

Hsu, T-C., Lu, C-H., Huang, Y-T., & Shih, W-P. (2011). Concentric polymer-dispersed liquid crystal rings for light intensity modulation. *Sensors and Actuators A-Physics*, *169*, 341–346.

Kachynski, A. V., Kuzmin, A. N., Prasad, P. N., & Smalyukh, I. I. (2008). Realignment-enhanced coherent anti-Stokes Raman scattering and three-dimensional imaging in anisotropic fluids. *Optics Express*, *16*, 10617–10632.

Khan, A., Khan, A. R., Salmieri, S., Tien, C. L., Riedl, B., Bouchard, J., et al. (2012). Mechanical and barrier properties of nanocrystalline cellulose reinforced chitosan based nanocomposite films. *Carbohydrate Polymers*, *90*, 1601–1608.

Kikuchi, H., Fujii, T., Kawakita, M., Fujikake, H., & Takizawa, K. (2000). Design and fabrication of a projection display using optically addressed polymer-dispersed liquid crystal light valves. *Optical Engineering*, *39*, 656–669.

Liu, Y. J., Ding, X., Lin, S-C. S., Shi, J., Chiang, I-K., & Huang, T. J. (2011). Surface acoustic wave driven light shutters using polymer-dispersed liquid crystals. *Advanced Materials*, *23*, 1656–1659.

Lovinger, A. J., Amundson, K. R., & Davis, D. D. (1994). Morphological investigation of UV-curable polymer-dispersed liquid crystal (PDLC) materials. *Chemistry of Materials*, *6*, 1726–1736.

Lv, K., Liu, D., Li, W., Tang, S., & Zhou, X. (2012). Preparation and characterization of E7–PMMA microcapsules by solvent evaporation. *Molecular Crystal & Liquid Crystals*, *557*, 217–227.

Marin, L., & Perju, E. (2008). New polymer-dispersed liquid crystals. Preparation and thermal characterization. *Metalurgia International*, 17–21. Special Issue: Exploring Romanian Resources in Materials Research.

Marin, L., & Perju, E. (2009). Polysulfone as polymer matrix for a novel polymer-dispersed liquid crystals system. *Phase Transition*, *82*, 507–518.

Marin, L., Simionescu, B. C., & Barboiu, M. (2012). Imino-chitosan biodynamers. *Chemical Communications*, *48*, 8778–8780.

Mucha, M. (2003). Polymer as an important component of blends and composites with liquid crystals. *Progress in Polymer Science*, *28*, 837–873.

Muzzarelli, R. A. A. (2009). Genipin–chitosan hydrogels as biomedical and pharmaceutical aids. *Carbohydrate Polymers*, *77*, 1–9.

Muzzarelli, R. A. A., Boudrant, J., Meyer, D., Manno, N., DeMarchis, M., & Paoletti, M. G. (2012). Current views on fungal chitin/chitosan, human chitinases, food preservation, glucans, pectins and inulin: A tribute to Henri Braconnot, precursor of the carbohydrate polymers science, on the chitin bicentennial. *Carbohydrate Polymers*, *87*, 995–1012.

Muzzarelli, R. A. A., Jeuniaux, C., & Gooday, G. W. (Eds.). (1986). *Chitin in nature and technology*. New York: Plenum Press.

Perju, E., Marin, L., Grigoras, V. C., & Bruma, M. (2011). Thermotropic and optical behaviour of new PDLC systems based on a polysulfone matrix and a cyanoazomethine liquid crystal. *Liquid Crystals*, *38*, 893–905.

Piryatinski, Y. P., & Yaroshchuk, O. V. (2000). Photoluminescence of pentylcyanobiphenyl in liquid crystal and solid crystal states. *Optics and Spectroscopy*, *89*, 860–866.

Ravi Kumar, M. N. V., Muzzarelli, R. A. A., Muzzarelli, C., Sashiwa, H., & Domb, A. J. (2004). Chitosan chemistry and pharmaceutical perspectives. *Chemical Reviews*, *104*, 6017–6084.

Ren, H. W., Fan, Y. H., Lin, Y. H., & Wu, S. T. (2005). Tunable-focus microlens arrays using nanosized polymer-dispersed liquid crystal droplets. *Optics Communications*, *247*, 101–106.

Russed, G. M., Paterson, B. J. A., Imrie, C. T., & Heeks, S. K. (1995). Thermal characterization of polymer dispersed liquid crystals by differential scanning calorimetry. *Chemistry of Materials*, *7*, 2185–2189.

Smith, G. W. (1993). Mixing and phase separation in liquid crystal/matrix systems: Determination of the excess specific heat of mixing. *Physical Review Letters*, *70*, 198–201.

Su, Y-C., Chu, C-C., Chang, W-T., & Hsiao, V. K. S. (2011). Characterization of optically switchable holographic polymer-dispersed liquid crystal transmission gratings. *Optical Materials*, *34*, 251–255.

Wang, J., Xia, J., Hong, S. W., Qiu, F., Yang, Y., & Lin, Z. (2007). Phase separation of polymer-dispersed liquid crystals on a chemically patterned substrate. *Langmuir*, *23*, 7411–7415.

White, T. J., Natarajan, L. V., Tondiglia, V. P., Bunning, T. J., & Guymon, C. A. (2007). Polymerization kinetics and monomer functionality effects in thiol–ene polymer dispersed liquid crystals. *Macromolecules*, *40*, 1112–1120.

Zhongqiang, Y., Jugal, K. G., Kenji, K., Yoshiko, S., Kato, T., & Abbott, N. L. (2010). Design of biomolecular interfaces using liquid crystals containing oligomeric ethylene glycol. *Advanced Functional Materials*, *9*, 2098–2106.

Zhou, J., Collard, D. M., Park, J. O., & Srinivasarao, M. (2002). Control of the anchoring behaviour of polymer-dispersed liquid crystal: Effect of branching in the side chains of polyacrylates. *Journal of American Chemical Society*, *124*, 9980–9981.

Zou, J., & Fang, J. (2011). Adhesive polymer-dispersed liquid crystal films. *Journal of Materials Chemistry*, *21*, 9149–9153.